Global Change Biology
celebrating 20 years
Global Change Biology (2014) **20**, 1674–1684, doi: 10.1111/gcb.12494

Allometric constraints on, and trade-offs in, belowground carbon allocation and their control of soil respiration across global forest ecosystems

GUANGSHUI CHEN[1,2], YUSHENG YANG[1] and DAVID ROBINSON[2]
[1]*Key Laboratory for Subtropical Mountain Ecology (Ministry of Science and Technology and Fujian Province Funded), School of Geographical Sciences, Fujian Normal University, Fuzhou 350007, China,* [2]*Institute of Biological & Environmental Sciences, School of Biological Sciences, University of Aberdeen, Aberdeen AB24 3UU, UK*

Abstract

To fully understand how soil respiration is partitioned among its component fluxes and responds to climate, it is essential to relate it to belowground carbon allocation, the ultimate carbon source for soil respiration. This remains one of the largest gaps in knowledge of terrestrial carbon cycling. Here, we synthesize data on gross and net primary production and their components, and soil respiration and its components, from a global forest database, to determine mechanisms governing belowground carbon allocation and their relationship with soil respiration partitioning and soil respiration responses to climatic factors across global forest ecosystems. Our results revealed that there are three independent mechanisms controlling belowground carbon allocation and which influence soil respiration and its partitioning: an allometric constraint; a fine-root production vs. root respiration trade-off; and an above- vs. belowground trade-off in plant carbon. Global patterns in soil respiration and its partitioning are constrained primarily by the allometric allocation, which explains some of the previously ambiguous results reported in the literature. Responses of soil respiration and its components to mean annual temperature, precipitation, and nitrogen deposition can be mediated by changes in belowground carbon allocation. Soil respiration responds to mean annual temperature overwhelmingly through an increasing belowground carbon input as a result of extending total day length of growing season, but not by temperature-driven acceleration of soil carbon decomposition, which argues against the possibility of a strong positive feedback between global warming and soil carbon loss. Different nitrogen loads can trigger distinct belowground carbon allocation mechanisms, which are responsible for different responses of soil respiration to nitrogen addition that have been observed. These results provide new insights into belowground carbon allocation, partitioning of soil respiration, and its responses to climate in forest ecosystems and are, therefore, valuable for terrestrial carbon simulations and projections.

Keywords: belowground carbon allocation, climate change, forest ecosystems, global warming, heterotrophic respiration, nitrogen deposition, root respiration, soil CO_2 efflux, soil respiration

Received 24 April 2013; revised version received 8 November 2013 and accepted 21 November 2013

Introduction

As the second largest carbon (C) flux between ecosystems and the atmosphere, soil respiration (R_s) releases 78–98 Gt C globally into the atmosphere each year, approximately an order of magnitude larger than the current annual fossil fuel emission (Bond-Lamberty & Thomson, 2010b; Hashimoto, 2012). Even minor changes in R_s potentially have strong feedbacks to atmospheric chemistry and global climate. For this reason, understanding the dynamics of and controls on R_s in a changing environment warrants serious attention.

R_s is a mixture of several CO_2 sources (Subke *et al.*, 2006). In practice, however, R_s is usually separated into heterotrophic respiration (R_h) and root respiration (R_r) using various techniques. A large body of literature has developed over the last two decades on the partitioning of R_s and how this is influenced by climatic drivers (Hanson *et al.*, 2000; Albanito *et al.*, 2012), but the underlying controls on partitioning remain unclear.

The C that comprises R_s comes ultimately from photosynthesis, i.e. gross primary production (GPP), but different components of R_s use C from distinct proximate sources (Chen *et al.*, 2011). For example, R_h originates from the microbial decomposition of accumulated soil organic matter (SOM) derived largely from repeated leaf and root litter inputs; R_r reflects the respiration of fine and coarse roots, and CO_2 produced during the breakdown of recent root exudates and rhizodeposits. Ecosystem process models suggest that variations in R_s and its components are sensitive to the belowground partitioning of photosynthesis (Thornton

Correspondence: Guangshui Chen, tel. +86 591 8348 3731, fax +86 591 8346 5397, e-mail: gschen@fjnu.edu.cn

et al., 2002). But fully characterizing the individual and collective controls on belowground C allocation (i.e. how GPP is allocated above- vs. belowground and among belowground components (Chen *et al.*, 2011)) remains an elusive goal despite this being fundamental to predicting R_s and its partitioning.

Previous studies of belowground C allocation have revealed some general patterns about total belowground C flux (TBCF; i.e. the total C used by fine roots, coarse roots, mycorrhizal growth, respiration, and root and mycorrhizal exudates; Giardina *et al.*, 2003, 2004; Ryan *et al.*, 2004; Litton *et al.*, 2007; Litton & Giardina, 2008; Ryan *et al.*, 2010; Vicca *et al.*, 2012). For example, less C is typically partitioned to TBCF with increasing GPP in forests from temperate to tropical regions (Litton *et al.*, 2007) and with increasing soil nutrient availability (Vicca *et al.*, 2012). Such insights have yet to be integrated into a comprehensive scheme to quantify how belowground C allocation is controlled and how those controls influence R_s and its variation with climate. This constitutes the largest gap in understanding terrestrial C cycling (Chapin *et al.*, 2009).

The responses of R_s and its heterotrophic component to climate, e.g., warming, precipitation, and atmospheric nitrogen (N) deposition (N_{dep}), are likely to influence feedbacks on climate by altering net terrestrial CO_2 flux. Climate can impact R_s directly through altering SOM decomposition rates, or indirectly via changes in the amount of photosynthate channeled belowground (Smith & Fang, 2010; Lu *et al.*, 2012). Without disaggregating the specific processes contributing to R_s, it is impossible to accurately predict the net response of soil C stores to climate variables and to identify feedbacks between them and C cycling processes.

To address these issues, we analyzed a global forest C flux database (Luyssaert *et al.*, 2007). This database, including 558 forests, contains information on C fluxes, ecosystem properties, and site information of forest stands. Data were collected from peer-reviewed literature, established databases, and personal communication with research groups involved in the regional networks of Fluxnet and associated projects (Luyssaert *et al.*, 2007). For this article, we extracted data on GPP and net primary production (NPP) and their components, and on R_s, R_h, and ancillary site information, to identify the most probable mechanisms of and controls on belowground C allocation and their influences on R_s, its partitioning, and responses to climate across forest ecosystems. GPP in those forests depends on a combination of allometric constraints on biomass production and a series of trade-offs between production components such as fine roots vs. wood, foliage vs. wood, and autotrophic respiration vs. production (Chen *et al.*, 2013). Here, we aimed to determine the following:

1 What are the mechanisms controlling belowground C allocation at large scales?
2 How are R_s and its partitioning related to belowground C allocation?
3 How does belowground C allocation mediate the responses of R_s and its components to climatic factors (temperature and precipitation) and N_{dep}?

Materials and methods

Data sets

The global forest database (Luyssaert *et al.*, 2007) is available online at http://www.ua.ac.be/main.aspx?c=sebastiaan.luyssaert&n=35884. For this study, three subsets of data were extracted from this database and listed as Tables S1, S2, and S3.

For these data, GPP was usually estimated via eddy covariance, component integration of NPP and plant autotrophic respiration (R_a), or process models [see Table S2 in Chen *et al.* (2013)]. Foliage production (NPP_{fl}) was determined by collecting leaf/needle fall plus any biomass increment. Coarse root production (NPP_{cr}) was determined mostly using species- and region-specific allometric equations (Luyssaert *et al.*, 2007). Both fine-root production (NPP_{fr}) and R_h were estimated by a variety of methods. Estimates of NPP_{fr} and R_h were selected from data obtained by a single method where estimates by different methods were simultaneously provided for the same site. The estimate of NPP_{fr} that was selected was determined by the 'quality' of the techniques used according to criteria defined by Wolf *et al.* (2010), i.e. when NPP_{fr} estimates were simultaneously provided by two or more techniques, only those obtained by the technique of the highest quality were included. The relative quality of the techniques used for estimating R_h is not known. However, soil trenching and root excision methods are the most commonly used approaches in studies included in the dataset. Estimates from only trenching or root excision studies were retained where estimates from other partitioning methods were also provided. R_r was derived as $R_s - R_h$ from which the R_r/R_s ratio was calculated. In addition to C flux data, climatic factors [mean annual temperature (MAT) and mean annual precipitation (MAP)], and wet, dry, and total N_{dep}, were also documented in the database.

Across latitudinal or altitudinal gradients MAT is not a single driving variable per se, but encompasses a multiplicity of factors such as radiation balance and length of growing season. We thus decomposed MAT into mean growing-season temperature (GST) and total day length (TDL) during the growing season for each site. To calculate GST, monthly air temperature of each site based on the CRU datasets (averaged from 1990 to 2002) was first linearly interpolated over an entire year to obtain 365 daily estimates of temperature. GST was then calculated by averaging daily temperatures that exceeded 0 °C. TDL during the growing season was estimated using the equation of Forsythe *et al.* (1995).

As with any meta-analysis, our risks were compromised by the limitations inherent to this approach. These are, first, the

uncertainties in, and technical limitations of, the methods used to obtain the original data. Second, even the most thorough and careful meta-analysis will inevitably contain biases, e.g., overestimation of effect size due to publication bias, inclusion of heterogeneous data and of poor quality studies, or confounding effects of unmeasured but influential environmental factors (Stewart, 2010). This bias can be magnified if analyses are based exclusively on one database. Third, although they provide the opportunity to study long-term climatic effects on ecosystem processes, the climate gradients that emerge from the collection of studies in databases such as that of Luyssaert *et al.* (2007) can provide fewer insights into the mechanisms of those processes and the identification of mechanisms if confounded by covarying factors (Dunne *et al.*, 2004; Rustad, 2008). Nevertheless, these potential weaknesses are often outweighed by the strong and important statistical relationships revealed by the meta-analytical approach that remain undetectable in individual studies (Fernandez-Duque & Valeggia, 1994; Cadotte *et al.*, 2012).

Data analysis

When multiple years of data were available, data were averaged over all years (Vicca *et al.*, 2012). All data were $\log_{10}$-transformed and the outliers of each variable were discarded in the following analysis. An outlier was defined as any data point more than 1.5 interquartile ranges below the first quartile or above the third quartile.

Because functional rather than predictive relationships were sought for the relationship between GPP and its components, the reduced major axis (RMA; Model Type II) regression (SMATR version 2.0; Warton *et al.*, 2006) was conducted to determine the allometric scaling relationship between GPP (x) and its components (y_i) using the form

$$\log(y_i) = \log(\alpha) + \beta \log(x)$$

where α is a constant and β the scaling exponent. Differences in RMA slopes were evaluated by likelihood ratio tests (Warton *et al.*, 2006).

Ordinary least square (OLS) linear regressions were conducted between GPP and R_s, R_h and R_r/R_s, and between GPP and its partitioning to NPP components. Differences in slopes of OLS regressions were tested by one-way analysis of covariance (ANCOVA).

At a steady state, soil C outputs (mainly R_s) should equal plant C inputs (mainly above- and belowground litter C for R_h, and recently assimilated C for R_r). Thus, a direct relationship between partitioning of R_s and partitioning among plant C sources is expected. However, some forest sites in this database have been disturbed recently or are relatively young and might not meet the strict steady-state assumption. Violation of this assumption would introduce some uncertainty into this relationship. As partitioning naturally implies trade-offs among components, we used a principal component analysis (PCA) to determine the form and identities of those trade-offs (Chen *et al.*, 2013). The database of Luyssaert *et al.* (2007) does not provide estimates of above- and belowground litter production, but we assumed that they could be approximated by NPP_{fl} and NPP_{fr}, respectively. The PCA was based on a correlation matrix of $\log_{10}$-transformed NPP_{fl}, NPP_{fr}, and R_r data. As the purpose of PCA in this study was to evaluate how these components were associated with each other and so to indicate possible trade-offs, but not to reduce dimensionality in the data, all the three principal component (PC) axes were saved. Leaf habits may affect the approximation of aboveground litterfall by NPP_{fl} and potentially influence the PCA results. Thus, a one-way analysis of variance (ANOVA) was also performed to test the significance of the effects of leaf habit on the PC scores. These analyses were done in SPSS 17.0 (SPSS Inc., Chicago, IL, USA).

To address how climatic factors directly and indirectly affect belowground C allocation, R_s and its partitioning, structural equation modeling (SEM) was applied. SEM is a widely used statistical technique that identifies which relationships among a complex series of interconnected variables are best correlated with data (McCune & Grace, 2002; Shipley, 2002; Antoninka *et al.*, 2009). The actual covariance structure of the dataset is compared with covariances generated by a structural model in which variables have hypothesized relationships with each other and which describes how they might influence one or more response variables (such as R_s). By sequentially eliminating from the models those relationships (or 'paths') between variables that are uncorrelated or weakly correlated, a parsimonious path structure is left which best explains the dependence of response variable(s) on others. This has the advantages of identifying interactions between multiple variables and distinguishing direct influences from indirect ones. Using information from the literature as the starting point, we hypothesized an *a priori* structure describing the possible influences of climatic variables on R_s, R_h or the R_r/R_s ratio (Fig. S1). To avoid bias due to the different numbers of sites per study, site-specific data from studies with multiple sites were down-weighted by the inverse of the corresponding number of sites (Ptacnik *et al.*, 2008). Maximum likelihood was used to estimate the standardized path coefficients in the SEM. To improve parsimony, the least significant path was deleted and the model was reestimated; then the next least significant path was removed, and so on, until the paths that remained in the final SEMs were all significant. The adequacy of the model was determined via χ^2 tests and the comparative fit index (CFI). Nonsignificant χ^2 tests ($P > 0.05$) and CFI values over 0.90 are considered acceptable (Shipley, 2002). The CFI assumes that all latent variables are uncorrelated (null/independence model) and compares the sample covariance matrix with this null model (Bentler, 1990). CFI is one of the most popularly reported fit indices because it is least affected by sample size. All structural equation modeling was conducted in AMOS 17.0 (SPSS Inc.).

Results

Allometric constraint on, and trade-offs in, belowground C allocation

The PCA analysis on belowground C fluxes shows that the first axis (PC1) explained 53% of the variance

Table 1 Loadings for, and percentage variation explained by, the three axes extracted by a principal components analysis (n = 78) on log-transformed belowground components of GPP, foliage production (NPP_{fl}), fine-root production (NPP_{fr}), and root respiration (R_r)

Component	PC1	PC2	PC3
Loading			
log NPP_{fl}	0.843	−0.025	−0.538
log NPP_{fr}	0.634	0.708	0.311
log R_r	0.686	−0.624	0.373
% of variance	52.8	29.7	17.5
Constraint or trade-off	Allometric constraint	NPP_{fr} vs. R_r trade-off	Above- vs. belowground trade-off

(Table 1). All the components of GPP were highly positively loaded. PC1 is essentially an axis of allometric increase in each component with GPP, representing the overriding allometric constraint on its belowground allocation. This was also shown by the RMA regressions in which all log-transformed components of GPP were significantly and positively related to log-transformed GPP (NPP_{cr} and R_r, Fig. 1a, b; NPP_{fl} and NPP_{fr}, Fig. 1a, d in Chen *et al.* (2013); Table S4).

The second PC axis (PC2), whose contribution to overall variance was 30%, had a positive correlation with NPP_{fr} and a negative correlation with R_r (Table 1). PC2 thus reflects a trade-off between root production and its respiratory cost.

The third axis (PC3), which explained 18% of the variance, was negatively correlated with NPP_{fl} and positively correlated with both the root components NPP_{fr} and R_r (Table 1). PC3 mainly represents an increasing C allocation to roots, at the expense of foliage production, i.e. an above- vs. belowground trade-off.

There was no significant effect of leaf habit on the PC scores (one-way ANOVA, $P > 0.05$ for all analyses; data

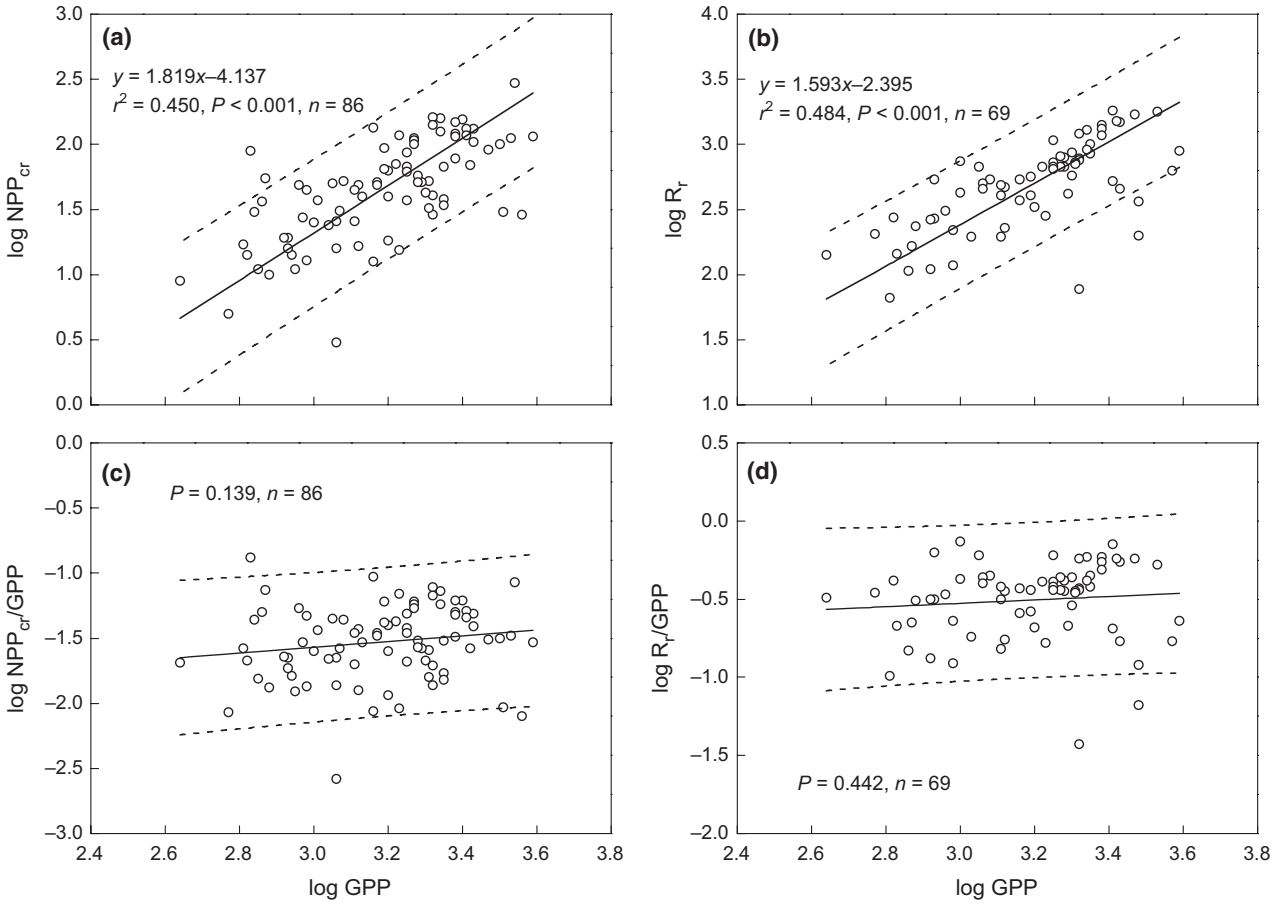

Fig. 1 Reduced major axis (RMA) regressions between log gross primary production (GPP) and log of its components (in g C m^{-2} yr^{-1}): (a) coarse root production (NPP_{cr}); and (b) root respiration (R_r). Ordinary least square (OLS) linear regressions between log of GPP and log of its partitioning to (c) NPP_{cr} and (d) R_r. Solid lines are regression curves and dashed lines denote prediction intervals.

not shown), indicating that the detected patterns of belowground C allocation were not an artifact caused by the approximating aboveground litterfall by NPP_{fl}.

R_s and its partitioning in relation to belowground C allocation

GPP explained nearly 70% of the variation in R_s (R^2 = 0.69; Fig. 2a). The R_s/GPP ratio varied from 0.3 to 1.0 (equivalent to log R_s/GPP ratios from −0.5 to 0.0; Fig. 2b), with a mean of 0.62, and decreased with increasing GPP. GPP explained 48% and 27% of the variation in R_r and R_h, respectively (Fig. 2c). Compared with R_r, R_h was less strongly dependent on GPP with a lower slope of the log–log regression (Fig. 2c) (one-way ANCOVA, $P < 0.001$; data not shown). Site-specific R_r/R_s varied from 0.20 to 0.83 (equivalent to log R_r/R_s ratios from −0.7 to −0.08: Fig. 2d) with a mean of 0.55, and increased with increasing GPP (Fig. 2d).

R_s was strongly and positively related to the PC1 axis, and varied negatively with PC2, as indicated by the final structural equation model (Fig. 3a). R_h was directly and positively affected by the PC1 axis and negatively by the PC3 axis (Fig. 3b). The R_r/R_s ratio was most affected by the PC2 axis, followed by the PC3 axis and the PC1 axis (Fig. 3c).

The positive effect of the PC1 axis on the R_r/R_s ratio results from the allometric allocation of GPP belowground. The scaling slope of log NPP_{fr} with log GPP is the lowest among component fluxes (Table S4). This results not only in a decreased partitioning of GPP to NPP_{fr} and relatively conservative partitioning to the other components as GPP increases (Fig. 1c, d; Fig. 1a, d in Chen *et al.* (2013)) but also causes a lag in the increase in R_h behind R_r (Fig. 2c), a decrease in R_s/GPP ratio (Fig. 2b), and an increase in the R_r/R_s ratio (Fig. 2d) with increasing GPP.

Effects of climatic factors on R_s and its components

Climatic factors had indirect effects on R_s and on its partitioning through their influences via the PC1 axis,

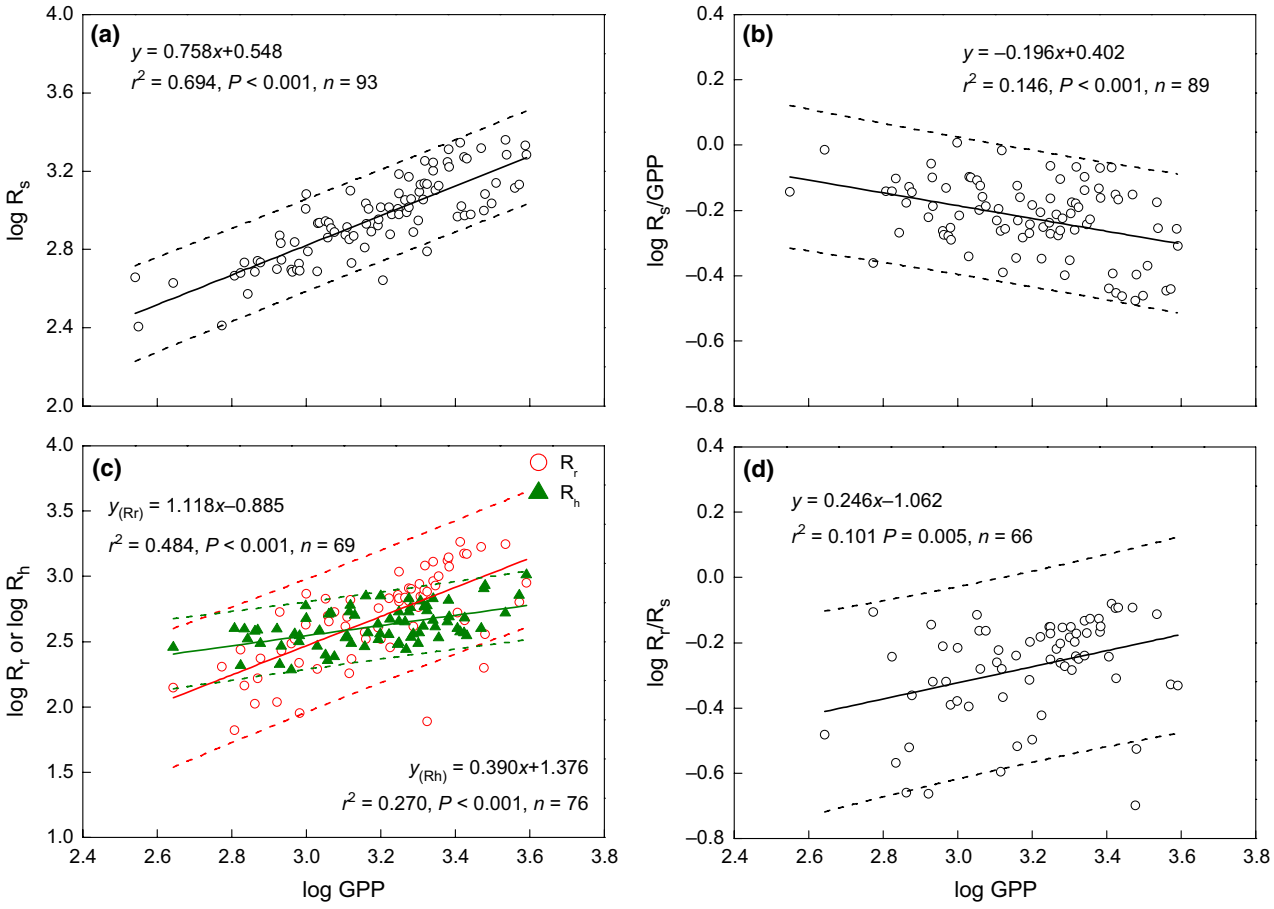

Fig. 2 Ordinary least square (OLS) linear regressions between log of gross primary production (GPP) and log of (a) soil respiration (R_s), (b) ratio of R_s to GPP, (c) root respiration (R_r, red), and heterotrophic respiration (R_h, green), and (d) the ratio of R_r to R_s (R_r/R_s). Solid lines are OLS regression curves and dashed lines denote prediction intervals.

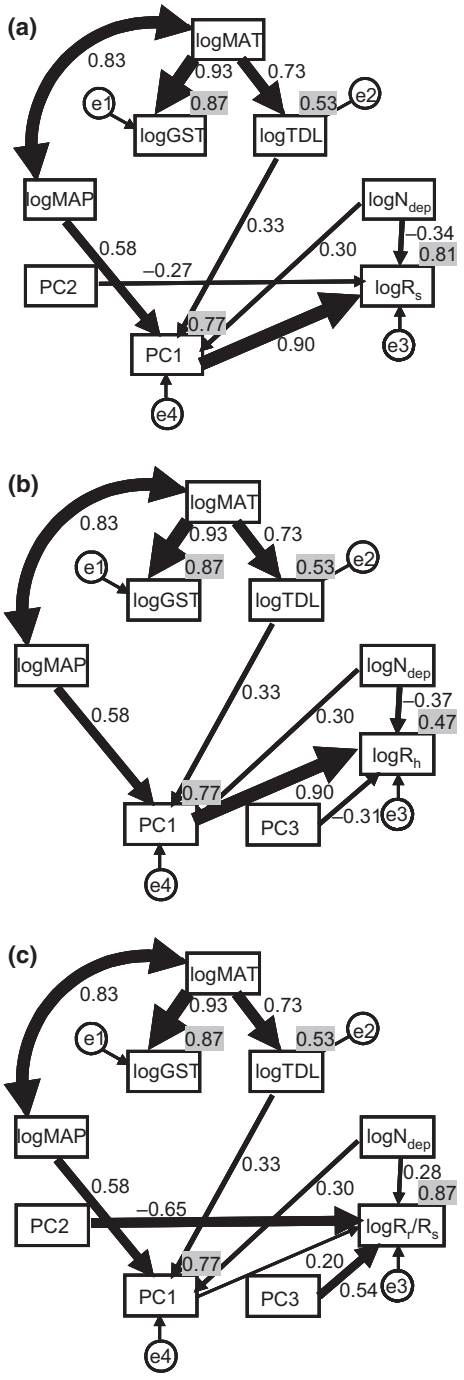

Fig. 3 The final structural equation model (SEM) of the effects of climatic factors and belowground C allocation on (a) soil respiration (R_s) ($\chi^2 = 15.529$, df = 19, $P = 0.688$, CFI = 1.000), (b) heterotrophic respiration (R_h) ($\chi^2 = 24.229$, df = 19, $P = 0.188$, CFI = 0.967), and (c) the root respiration (R_r) to R_s ratio (R_r/R_s) ($\chi^2 = 26.741$, df = 26, $P = 0.423$, CFI = 0.996). $n = 78$ for all analyses. Measured variables are represented by boxes. Circles indicate error terms (e1–e4). Causal relationships and covariations are represented by one-headed and double-headed arrows, respectively. The thickness of the arrows is proportional to the magnitude of the standardized path coefficients or covariation coefficients, which are all statistically significant ($P < 0.05$) and indicated by the numbers on the arrows. Numbers in shaded boxes adjacent to a dependent variable are the proportions of variance in this dependent variable explained by its independent variables (R^2). MAT, mean annual air temperature; TDL, total day length of growing season; MAP, mean annual precipitation; N_{dep}, atmospheric nitrogen deposition; PC1, PC2, and PC3 are the three principal components in Table 1, indicating the allometrically constrained belowground input, a NPP_{fr} vs. R_r trade-off, and an above- vs. belowground trade-off.

which reflects the allometric constraint on belowground C allocation (Fig. 3a–c). Both MAT and MAP had positive net effects on R_s, R_h, and the R_r/R_s ratio (Table 2). However, the effect of MAT was mediated overwhelmingly by TDL, but not by GST (Fig. 3; Table 2). N_{dep} had negative direct effects on R_s and R_h and a positive direct effect on R_r/R_s, while it had positive indirect effects on all three via PC1 (Table 2).

Discussion

What are the mechanisms controlling belowground C allocation?

There are multiple controls on belowground C allocation across global forest ecosystems: the allometric constraint (PC1), and two trade-offs, i.e. the NPP_{fr} vs. R_r trade-off (PC2) and the above- vs. belowground trade-off (PC3) (Fig. 4a). In most vegetation models, however, belowground C allocation is described only by simple assumed mechanisms. These include defining the relationship between above- and belowground production with a single allometric relation (e.g., ED, SEIBDGVM) or that for the above- vs. belowground trade-off according to soil water or nutrient limitations (e.g., O-CN, LPJ, LPJGUESS, aDGVM, sDGVM, CLM-CN, and ORCHIDEE) (Metcalfe *et al.*, 2011). Many models allocate plant C according to simple phenomenological rules that can be traced to the equations in Friedlingstein *et al.* (1999). Those equations include terms analogous to the allometric constraint and to the above- vs. belowground trade-off in C allocation identified in our analysis. It should be possible to replace the assumed constants in those equations with the more precise functions derived from our analysis to reflect the multiplicity of controls on C allocation that occur in real ecosystems.

Not all the mechanisms implied by Fig. 4a will function equally in a specific setting. There is likely to be one or more dominant mechanisms depending on the spatial or temporal scales considered and on local environmental conditions. In this study, belowground C allocation was controlled primarily by the allometric

Table 2 Total direct and indirect effects in the final structural equation models (Fig. 3) expressed as standardized path coefficients. A direct effect is simply the path coefficient from one variable to another; an indirect effect is the product of all the path coefficients along the sequence of paths through one or more intermediate variables; and a total effect is the sum of the relevant direct and indirect effects. All paths were significant ($P < 0.05$)

	log MAT	log TDL	log MAP	log N_{dep}	PC1	PC2	PC3
Total effects							
PC1	0.239	0.330	0.585	0.304	–	–	–
log R_s	0.214	0.295	0.523	−0.072	0.895	−0.273	–
log R_h	0.146	0.201	0.356	−0.188	0.609	–	−0.314
log R_r/R_s	0.048	0.066	0.117	0.343	0.201	−0.654	0.537
Direct effects							
PC1	–	0.33	0.585	0.304	–	–	–
log R_s	–	–	–	−0.344	0.895	−0.273	–
log R_h	–	–	–	−0.373	0.609	–	−0.314
log R_r/R_s	–	–	–	0.282	0.201	−0.654	0.537
Indirect effects							
PC1	0.239	–	–	–	–	–	–
log R_s	0.214	0.295	0.523	0.272	–	–	–
log R_h	0.146	0.201	0.356	0.185	–	–	–
log R_r/R_s	0.048	0.066	0.117	0.061	–	–	–

R_s, soil respiration; R_h, heterotrophic respiration; R_r/R_s, the root respiration (R_r) to R_s ratio; MAT, mean annual air temperature; TDL, total day length of growing season; MAP, mean annual precipitation; N_{dep}, atmospheric nitrogen deposition; PC1, PC2, and PC3 are the three principal components in Table 1, indicating the allometrically constrained belowground input, a NPP_{fr} vs. R_r trade-off, and an above- vs. belowground trade-off.

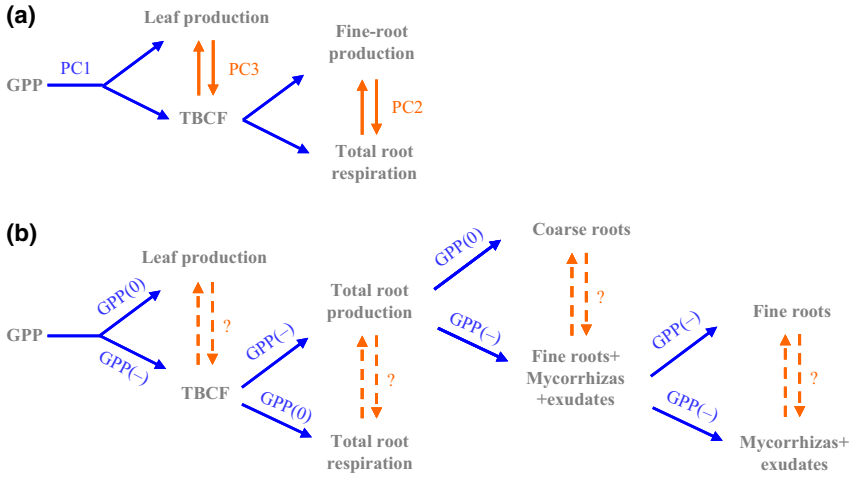

Fig. 4 (a) Belowground C allocation patterns evidenced by a principle component analysis, where allometric allocation (i.e. PC1 in Table 1) is indicated by blue single arrows; a fine-root production vs. root respiration trade-off (i.e. PC2) and an above- vs. belowground trade-off (i.e. PC3) both indicated by orange solid double arrows. (b) A hypothesized scheme for integrating the components of belowground C allocation. C allocation is governed both by allometric constraints on how GPP is partitioned, indicated as blue single arrows, and possible trade-offs among belowground components, indicated by orange broken double arrows and with '?'. The '−' and '0' in the round brackets following 'GPP' on an arrow, respectively, indicate decreasing or unchanged partitioning of GPP to a component with increasing GPP. GPP, gross primary productivity; TBCF, total belowground carbon flux.

constraint and secondarily by the two trade-offs across the global scale (Table 1). However, across a North American gradient of boreal *Picea mariana* (black spruce) forests where GPP is near-constant, total belowground C flux (TBCF) has a negative relationship with aboveground NPP (Vogel *et al.*, 2008), indicating that the above- vs. belowground trade-off might predominate. In intraspecific experiments such trade-off can also override effects of the allometric constraint (McDowell *et al.*, 2001; Palmroth *et al.*, 2006).

It should be stressed that the patterns indicated in Fig. 4(a) are a simplified version of belowground C allocation. Due to the inevitably incomplete measurement of belowground C components such as mycorrhizal fungi and exudates, which can consume a significant fraction of TBCF (Kuzyakov & Cheng, 2001; Högberg & Högberg, 2002; Robinson, 2004; Fahey *et al.*, 2005), a comprehensive examination of the mechanisms controlling belowground C allocation was not possible. Nonetheless, on the basis of present analysis and previous literature, we can construct a more detailed mechanistic description of belowground allometric partitioning at the global scale from which certain predictions arise (Fig. 4b). Both Litton *et al.* (2007) and this study predict that an increase in GPP would decrease the partitioning to TBCF, but partitioning to leaf production would remain constant. As C allocation to ectomycorrhizal fungi and root exudates is positively correlated with belowground C allocation (Hobbie, 2006; Phillips *et al.*, 2008), decreased partitioning to TBCF with increasing GPP should, therefore, cascade into a decreased partitioning to mycorrhizas and exudates. Together with a decreased partitioning to fine-root production revealed in the current analysis, total C partitioned to structures and processes responsible for the exploitation of soil resources, i.e. fine roots, mycorrhizas, and exudates, would decrease with increasing GPP, contrasting with the partitioning to coarse root production, which remains relatively constant. Partitioning to total root production would thus decrease with increasing GPP, compared with a relatively conservative partitioning to total root respiration (Fig. 4b).

By comparison, we currently know much less about the possible trade-offs among belowground components (Fig. 4b). However, there might be a trade-off among C allocation for soil resource exploitation (Brundrett, 2002; Fischer *et al.*, 2007; Felderer *et al.*, 2013), reflecting a shifting balance between the reliance of plants on fine roots vs. mycorrhizas plus exudates (Fig. 4b). As Giardina *et al.* (2004) observed shifted belowground C allocation from fine roots and mycorrhizal hyphae toward coarse roots with increased nutrient supply in a *Eucalyptus* plantation, there also likely exists a fine roots plus mycorrhizas plus exudates vs. coarse roots trade-off (Fig. 4b), which might reflect the 'fine roots vs. wood' trade-off we found previously (Chen *et al.*, 2013). There is also a probable root production vs. root respiration trade-off that corresponds to the 'total plant production vs. plant respiration trade-off' identified in Chen *et al.* (2013). The NPP_{fr} vs. R_r trade-off (PC2) that we have found (Fig. 4a) could be simply a combination of possible trade-offs between fine vs. coarse roots and root production vs. root respiration (Fig. 4b). According to Chen *et al.* (2013), there is no direct trade-off between leaves and fine roots nor between above- and belowground parts. Instead, foliage or fine roots both trade-off independently with wood. Thus, the above- vs. belowground trade-off (PC3) (Fig. 4a) detected here would be an effect of these two independent trade-offs. Ideally, separately estimating all the component fluxes above- and belowground would clarify the detailed controls on belowground C allocation, but the practical difficulties of doing so remain formidable.

How can R_s and its partitioning be related to belowground C allocation?

The significant relationship of R_s and its components to GPP (Fig. 2a, c) strengthens the evidence for the close coupling of R_s to current photosynthesis (Davidson *et al.*, 2006; Högberg & Read, 2006; Kuzyakov & Gavrichkova, 2010). Ours is the first study to relate R_s and its components to GPP directly measured *in situ* across a global range of forest types, rather than to proxies of GPP (e.g., litterfall, fine-root biomass) (Raich & Nadelhoffer, 1989; Janssens *et al.*, 2001; Davidson *et al.*, 2002; Bond-Lamberty & Thomson, 2010a; Sheng *et al.*, 2010; Caprez *et al.*, 2012) or modeled GPP (Vargas *et al.*, 2010). These relationships will greatly facilitate the prediction of R_s and its components from estimates of GPP obtained from models of canopy photosynthesis combined with biophysical information derived from remote sensing (e.g., Running *et al.*, 2004). The allometric constraint on belowground C allocation is the main reason for the close coupling of R_s and its components with GPP and for the positive correlation between R_h and R_r across a wide range of forests (Bond-Lamberty *et al.*, 2004).

It is notable that the variation in R_h with GPP was weaker than that of R_r, as indicated by the much lower slope (<1.0) and smaller R^2 of the ln R_h on ln GPP regression (Fig. 2c). This pattern is predictable from the differences in accessibility and availability of the C sources for R_h and R_r, and the dissimilar timescales with which their production rates depend on GPP (Trumbore & Czimczik, 2008). The immediate C sources for R_r are derived from recent photosynthate (Högberg & Read, 2006; Subke *et al.*, 2011), the rate of which reflects NPP and, hence, GPP. The C sources for R_h include some relatively labile organic matter (fresh leaf and fine-root litter), but comprise mostly older, more recalcitrant and structurally heterogeneous SOM (Schmidt *et al.*, 2011), the production rates of which relate far less strongly to current GPP. In addition, Litton *et al.* (2007) reported a decreasing partitioning of GPP to TBCF with increasing GPP. Our analysis suggests that this trend could arise from a decreasing

partitioning of C to NPP_{fr}, because partitioning to other components (NPP_{cr} and R_r) remains relatively constant (Fig. 1). This belowground partitioning pattern also contributes to the lower slope of the relationship between R_h and GPP compared with that between R_r and GPP. It also explains the decreasing R_s/GPP ratio and increasing R_r/R_s ratio with increasing GPP (Fig. 2) and the positive relationships between R_r/R_s and R_s reported in previous global syntheses (Bond-Lamberty *et al*., 2004; Subke *et al*., 2006).

A negative association between the NPP_{fr} vs. R_r trade-off (PC2) and R_s would arise because of increasing partitioning of C to NPP_{fr}, which is generally considered to be more effective than foliar litter in building up SOM stocks (Rasse *et al*., 2005), is likely to eventually enhance the percentage of GPP sequestered as SOM and will tend to correspondingly reduce CO_2 loss via R_s. Importantly, we found that the strongest influence on partitioning of R_s at the global scale was the NPP_{fr} vs. R_r trade-off (PC2) (Fig. 3c). Understanding the partitioning of TBCF is thus not only critical to soil C sequestration but also to the partitioning of R_s, as pointed out by Chapin *et al.* (2009).

The above- vs. belowground trade-off (PC3) is negatively related to R_h but has a nonsignificant effect on R_s (Fig. 3). This is because greater belowground allocation of plant-derived C will increase partitioning to R_r and decrease that to R_h (Chen *et al*., 2011), but will not reduce the total surface CO_2 flux, R_s. It is also for this reason that the above- vs. belowground trade-off (PC3) has a positive effect on the R_r/R_s ratio.

How can belowground C allocation mediate the responses of R_s and its components to climate and N_{dep}?

The annual global R_s increased at 0.1 Pg C yr^{-1} (or 0.1% yr^{-1}) between 1989 and 2008 (Bond-Lamberty & Thomson, 2010b). This has aroused concern about the possible positive feedbacks between the C cycle and planetary warming, a prediction of many climate models (Cao & Woodward, 1998; Cox *et al*., 2000; Friedlingstein *et al*., 2006). However, there is controversy about the underlying processes, in particular if it is primarily elevated temperature or stimulated assimilate supply that is driving the global R_s increase (Smith & Fang, 2010).

Our analysis helps to resolve this controversy. We found that the apparent effects of MAT on R_s and R_h are not direct influences on these processes, but are mediated indirectly via those of total day length (TDL) on belowground C allocation (i.e. PC1). This carries the strong implication that, over the long-term, R_s and its heterotrophic components are constrained ultimately by assimilate supply from vegetation, but not by temperature. It follows that the increase in global R_s during the past few decades (Bond-Lamberty & Thomson, 2010b) has, therefore, probably been caused primarily by larger global GPP stimulated by extended TDL, but not from a temperature-accelerated decomposition of SOM. This cautions against the assumption of strong positive feedbacks between increased R_s and global warming (Cao & Woodward, 1998; Cox *et al*., 2000; Friedlingstein *et al*., 2006).

Mean growing-season temperature (GST) had no effect on the PC1 axis, i.e. on allometric belowground C inputs. This is consistent with Kerkhoff *et al.* (2005) and Enquist *et al.* (2007) who found that forest production has no relationship with GST after it is adjusted for differences in TDL. This temperature insensitivity was attributed to adaptive differences in tree growth rates across temperature gradients (Enquist *et al*., 2007).

The net effects of MAP on R_s and R_h at the global scale are positive, which is consistent with previous studies, e.g., Raich *et al.* (2002) and Reichstein *et al.* (2003). This effect was mediated by increases in litter and root C input (i.e. PC1), probably as a result of precipitation-stimulated plant production (Luyssaert *et al*., 2007).

There appear to be two countervailing effects of N_{dep} on R_s and R_h. The positive but indirect effect was mediated by the allometric constraint on belowground C allocation (PC1), such that additional N would stimulate litter and root C inputs, an effect though clearly detectable at the global scale, has not often been observed in N deposition experiments (Pregitzer *et al*., 2008; Janssens *et al*., 2010). This discrepancy might be related to the much higher N loading rate in N deposition experiments than that of ambient N_{dep}. In a boreal forest, Hasselquist *et al.* (2012) found that mean R_s was 50% greater in a low N treatment (20 kg N ha^{-1} yr^{-1}) than in either an unfertilized control or high N treatment (100 kg N ha^{-1} yr^{-1}). If the above- vs. belowground trade-off (PC3) is triggered under a high N load, an increase in aboveground litter input will likely be counteracted by decreased belowground C allocation resulting in no significant net effect on R_s. However, N_{dep} is usually at a rate around one fifth of that applied in typical fertilization experiments (Hasselquist *et al*., 2012). The simulated N deposition rates (30 kg N ha^{-1} yr^{-1}) in Pregitzer *et al.* (2008) was the lowest among the studies included in the meta-analysis of Janssens *et al.* (2010), but was still three times higher than the ambient N_{dep} of the study site. The sites included in our study received N_{dep} at rates (2.3–27 kg N ha^{-1} yr^{-1}), comparable with the low N treatment in Hasselquist *et al.* (2012). Such a low N_{dep} would probably induce an allometric increase in litter and root C inputs instead of an

above- vs. belowground trade-off (Janssens *et al.*, 2010). The negative direct effect of N_{dep} on R_s and R_h could be associated with the frequently reported decreased rates of plant litter and SOM decomposition in systems exposed to N deposition (Janssens *et al.*, 2010).

Among individual experiments, the net effect of N_{dep} on R_s has been inconsistent, with N_{dep} sometimes increasing R_s, sometimes decreasing it, or having no measurable effect (Janssens *et al.*, 2010). Our analysis offers an obvious explanation for this inconsistency: it arises from variations, perhaps site- or season-specific, in the balance between the direct negative and indirect positive effects of N_{dep} (Fig. 3a).

In conclusion, there are three distinct, but related, mechanisms controlling belowground C allocation and which influence R_s: allometric C allocation; an NPP_{fr} vs. R_r trade-off; and an above- vs. belowground trade-off in plant C. While global patterns in R_s and its components are constrained primarily by the allometries of belowground C components, all three belowground allocation mechanisms exert quantitatively different and variable influences on R_s and its partitioning. This explains some of the previously ambiguous results reported in the literature. Responses of R_s and its components to MAT, MAP, and N_{dep} can be mediated by changes in belowground C allocation. R_s responds to MAT principally through an increasing belowground C input as a result of extending TDL, but not by temperature-driven acceleration of SOM decomposition. Different N loads can trigger distinct belowground C allocation mechanisms. Together with N-inhibited SOM decomposition, these mechanisms are responsible for different responses of R_s to N addition that have been observed. Incorporating information about belowground C allocation in both experimental and modeling studies should therefore produce a more comprehensive picture of the controls on R_s and its response to climate.

Acknowledgements

We thank all site investigators, their funding agencies, the various regional flux networks (Afriflux, AmeriFlux, AsiaFlux, CarboAfrica, CarboEurope-IP, ChinaFlux, Fluxnet-Canada, KoFlux, LBA, NECC, OzFlux, TCOS-Siberia, USCCC), and the Fluxnet project, whose support is essential for obtaining the measurements without which the type of integrated analyses conducted in this study would not be possible. The research was funded by the National Natural Science Foundation of China (Nos. 31130013 and 30972347), the Program for Changjiang Scholars and Innovative Research Team in University (PCSIRT) (No. IRT0960), and the Science Foundation of the Fujian Province, China (No. 2010J06009). We also thank Fabrizio Albanito and three anonymous referees for their helpful suggestions and comments on the manuscript.

References

Albanito F, Mcallister JL, Cescatti A, Smith P, Robinson D (2012) Dual-chamber measurements of $\delta^{13}C$ of soil-respired CO_2 partitioned using a field-based three end-member model. *Soil Biology and Biochemistry*, **47**, 106–115.

Antoninka A, Wolf JE, Bowker M, Classen AT, Johnson NC (2009) Linking above- and belowground responses to global change at community and ecosystem scales. *Global Change Biology*, **15**, 914–929.

Bentler PM (1990) Comparative fit indexes in structural models. *Psychological bulletin*, **107**, 238–247.

Bond-Lamberty B, Thomson A (2010a) A global database of soil respiration data. *Biogeosciences*, **7**, 1915–1926.

Bond-Lamberty B, Thomson A (2010b) Temperature-associated increases in the global soil respiration record. *Nature*, **464**, 579–582.

Bond-Lamberty B, Wang C, Gower ST (2004) A global relationship between the heterotrophic and autotrophic components of soil respiration? *Global Change Biology*, **10**, 1756–1766.

Brundrett MC (2002) Coevolution of roots and mycorrhizas of land plants. *New Phytologist*, **154**, 275–304.

Cadotte MW, Mehrens LR, Menge DNL (2012) Gauging the impact of meta-analysis on ecology. *Evolutionary Ecology*, **26**, 1153–1167.

Cao M, Woodward FI (1998) Dynamic responses of terrestrial ecosystem carbon cycling to global climate change. *Nature*, **393**, 249–252.

Caprez R, Niklaus P, Körner C (2012) Forest soil respiration reflects plant productivity across a temperature gradient in the Alps. *Oecologia*, **170**, 1143–1154.

Chapin FS, Mcfarland J, Mcguire AD, Euskirchen ES, Ruess RW, Kielland K (2009) The changing global carbon cycle: linking plant-soil carbon dynamics to global consequences. *Journal of Ecology*, **97**, 840–850.

Chen G, Yang Y, Guo J, Xie J, Yang Z (2011) Relationships between carbon allocation and partitioning of soil respiration across world mature forests. *Plant Ecology*, **212**, 195–206.

Chen G, Yang Y, Robinson D (2013) Allocation of gross primary production in forest ecosystems: allometric constraints and envionmental responses. *New Phytologist*, **200**, 1176–1186.

Cox PM, Betts RA, Jones CD, Spall SA, Totterdell IJ (2000) Acceleration of global warming due to carbon-cycle feedbacks in a coupled climate model. *Nature*, **408**, 184–187.

Davidson EA, Savage K, Bolstad P *et al.* (2002) Belowground carbon allocation in forests estimated from litterfall and IRGA-based soil respiration measurements. *Agricultural and Forest Meteorology*, **113**, 39–51.

Davidson EA, Janssens IA, Luo Y (2006) On the variability of respiration in terrestrial ecosystems: moving beyond Q_{10}. *Global Change Biology*, **12**, 154–164.

Dunne JA, Saleska SR, Fischer ML, Harte J (2004) Integrating experimental and gradient methods in ecological climate change research. *Ecology*, **85**, 904–916.

Enquist BJ, Kerkhoff AJ, Huxman TE, Economo EP (2007) Adaptive differences in plant physiology and ecosystem paradoxes: insights from metabolic scaling theory. *Global Change Biology*, **13**, 591–609.

Fahey TJ, Tierney GL, Fitzhugh RD, Wilson GF, Siccama TG (2005) Soil respiration and soil carbon balance in a northern hardwood forest ecosystem. *Canadian Journal of Forest Research*, **35**, 244–253.

Felderer B, Jansa J, Schulin R (2013) Interaction between root growth allocation and mycorrhizal fungi in soil with patchy P distribution. *Plant and Soil*, **373**, 569–582.

Fernandez-Duque E, Valeggia C (1994) Meta-analysis: a valuable tool in conservation research. *Conservation Biology*, **8**, 555–561.

Fischer DG, Hart SC, Leroy CJ, Whitham TG (2007) Variation in below-ground carbon fluxes along a Populus hybridization gradient. *New Phytologist*, **176**, 415–425.

Forsythe WC, Rykiel EJ Jr, Stahl RS, Wu H-I, Schoolfield RM (1995) A model comparison for daylength as a function of latitude and day of year. *Ecological Modelling*, **80**, 87–95.

Friedlingstein P, Joel G, Field CB, Fung IY (1999) Toward an allocation scheme for global terrestrial carbon models. *Global Change Biology*, **5**, 755–770.

Friedlingstein P, Cox P, Betts R *et al.* (2006) Climate–carbon cycle feedback analysis: results from the C4MIP model intercomparison. *Journal of Climate*, **19**, 3337–3353.

Giardina C, Ryan M, Binkley D, Fownes J (2003) Primary production and carbon allocation in relation to nutrient supply in a tropical experimental forest. *Global Change Biology*, **9**, 1438–1450.

Giardina C, Binkley D, Ryan M, Fownes J, Senock R (2004) Belowground carbon cycling in a humid tropical forest decreases with fertilization. *Oecologia*, **139**, 545–550.

Hanson PJ, Edwards NT, Garten CT, Andrews JA (2000) Separating root and soil microbial contributions to soil respiration: a review of methods and observations. *Biogeochemistry*, **48**, 115–146.

Hashimoto S (2012) A new estimation of global soil greenhouse gas fluxes using a simple data-oriented model. *PLoS ONE*, **7**, e41962.
Hasselquist NJ, Metcalfe DB, Högberg P (2012) Contrasting effects of low and high nitrogen additions on soil CO_2 flux components and ectomycorrhizal fungal sporocarp production in a boreal forest. *Global Change Biology*, **18**, 3596–3605.
Hobbie EA (2006) Carbon allocation to ectomycorrhizal fungi correlates with belowground allocation in culture studies. *Ecology*, **87**, 563–569.
Högberg MN, Högberg P (2002) Extramatrical ectomycorrhizal mycelium contributes one-third of microbial biomass and produces, together with associated roots, half the dissolved organic carbon in a forest soil. *New Phytologist*, **154**, 791–795.
Högberg P, Read DJ (2006) Towards a more plant physiological perspective on soil ecology. *Trends in Ecology & Evolution*, **21**, 548–554.
Janssens IA, Lankreijer H, Matteucci G *et al.* (2001) Productivity overshadows temperature in determining soil and ecosystem respiration across European forests. *Global Change Biology*, **7**, 269–278.
Janssens IA, Dieleman W, Luyssaert S *et al.* (2010) Reduction of forest soil respiration in response to nitrogen deposition. *Nature Geoscience*, **3**, 315–322.
Kerkhoff AJ, Enquist BJ, Elser JJ, Fagan WF (2005) Plant allometry, stoichiometry and the temperature-dependence of primary productivity. *Global Ecology and Biogeography*, **14**, 585–598.
Kuzyakov Y, Cheng W (2001) Photosynthesis controls of rhizosphere respiration and organic matter decomposition. *Soil Biology and Biochemistry*, **33**, 1915–1925.
Kuzyakov Y, Gavrichkova O (2010) Review: time lag between photosynthesis and carbon dioxide efflux from soil: a review of mechanisms and controls. *Global Change Biology*, **16**, 3386–3406.
Litton CM, Giardina CP (2008) Below-ground carbon flux and partitioning: global patterns and response to temperature. *Functional Ecology*, **22**, 941–954.
Litton CM, Raich JW, Ryan MG (2007) Carbon allocation in forest ecosystems. *Global Change Biology*, **13**, 2089–2109.
Lu M, Zhou X, Yang Q *et al.* (2012) Responses of ecosystem carbon cycle to experimental warming: a meta-analysis. *Ecology*, **94**, 726–738.
Luyssaert S, Inglima I, Jung M *et al.* (2007) CO_2 balance of boreal, temperate, and tropical forests derived from a global database. *Global Change Biology*, **13**, 2509–2537.
McCune B, Grace JB (2002) *Analysis of Ecological Communities*. MjM Software Design, Gleneden Beach, OR, USA.
McDowell NG, Balster NJ, Marshall JD (2001) Belowground carbon allocation of Rocky Mountain Douglas-fir. *Canadian Journal of Forest Research*, **31**, 1425–1436.
Metcalfe DB, Fisher RA, Wardle DA (2011) Plant communities as drivers of soil respiration: pathways, mechanisms, and significance for global change. *Biogeosciences*, **8**, 2047–2061.
Palmroth S, Oren R, Mccarthy HR *et al.* (2006) Aboveground sink strength in forests controls the allocation of carbon below ground and its $[CO_2]$-induced enhancement. *Proceedings of the National Academy of Sciences*, **103**, 19362–19367.
Phillips RP, Erlitz Y, Bier R, Bernhardt ES (2008) New approach for capturing soluble root exudates in forest soils. *Functional Ecology*, **22**, 990–999.
Pregitzer KS, Burton AJ, Zak DR, Talhelm AF (2008) Simulated chronic nitrogen deposition increases carbon storage in Northern Temperate forests. *Global Change Biology*, **14**, 142–153.
Ptacnik R, Solimini AG, Andersen T *et al.* (2008) Diversity predicts stability and resource use efficiency in natural phytoplankton communities. *Proceedings of the National Academy of Sciences*, **105**, 5134–5138.
Raich JW, Nadelhoffer KJ (1989) Belowground carbon allocation in forest ecosystems: global trends. *Ecology*, **70**, 1346–1354.
Raich JW, Potter CS, Bhagawati D (2002) Interannual variability in global soil respiration, 1980–94. *Global Change Biology*, **8**, 800–812.
Rasse DP, Rumpel C, Dignac MF (2005) Is soil carbon mostly root carbon? Mechanisms for a specific stabilisation. *Plant and Soil*, **269**, 341–356.
Reichstein M, Rey A, Freibauer A *et al.* (2003) Modeling temporal and large-scale spatial variability of soil respiration from soil water availability, temperature and vegetation productivity indices. *Global Biogeochemical Cycles*, **17**, 1104.
Robinson D (2004) Scaling the depths: below-ground allocation in plants, forests and biomes. *Functional Ecology*, **18**, 290–295.
Running SW, Nemani RR, Heinsch FA, Zhao MS, Reeves M, Hashimoto H (2004) A continuous satellite-derived measure of global terrestrial primary production. *BioScience*, **54**, 547–560.
Rustad LE (2008) The response of terrestrial ecosystems to global climate change: towards an integrated approach. *Science of the Total Environment*, **404**, 222–235.
Ryan MG, Binkley D, Fownes JH, Giardina CP, Senock RS (2004) An experimental test of the causes of forest growth decline with stand age. *Ecological Monographs*, **74**, 393–414.
Ryan MG, Stape JL, Binkley D *et al.* (2010) Factors controlling Eucalyptus productivity: how water availability and stand structure alter production and carbon allocation. *Forest Ecology and Management*, **259**, 1695–1703.
Schmidt M, Torn MS, Abiven S *et al.* (2011) Persistence of soil organic matter as an ecosystem property. *Nature*, **479**, 49–56.
Sheng H, Yang Y, Yang Z, Chen G, Xie J, Guo J, Zou S (2010) The dynamic response of soil respiration to land-use changes in subtropical China. *Global Change Biology*, **16**, 1107–1121.
Shipley B (2002) *Cause and Correlation in Biology – A User's Guide to Path Analysis, Structural Equations and Causal Inference*. Cambridge University Press, Cambridge, UK.
Smith P, Fang CM (2010) Carbon cycle: a warm response by soils. *Nature*, **464**, 499–500.
Stewart G (2010) Meta-analysis in applied ecology. *Biology Letters*, **6**, 78–81.
Subke J-A, Inglima I, Francesca Cotrufo M (2006) Trends and methodological impacts in soil CO_2 efflux partitioning: a metaanalytical review. *Global Change Biology*, **12**, 921–943.
Subke J-A, Voke NR, Leronni V, Garnett MH, Ineson P (2011) Dynamics and pathways of autotrophic and heterotrophic soil CO_2 efflux revealed by forest girdling. *Journal of Ecology*, **99**, 186–193.
Thornton PE, Law BE, Gholz HL *et al.* (2002) Modeling and measuring the effects of disturbance history and climate on carbon and water budgets in evergreen needleleaf forests. *Agricultural and Forest Meteorology*, **113**, 185–222.
Trumbore SE, Czimczik CI (2008) An uncertain future for soil carbon. *Science*, **321**, 1455–1456.
Vargas R, Baldocchi DD, Allen MF *et al.* (2010) Looking deeper into the soil: biophysical controls and seasonal lags of soil CO_2 production and efflux. *Ecological Applications*, **20**, 1569–1582.
Vicca S, Luyssaert S, Peñuelas J *et al.* (2012) Fertile forests produce biomass more efficiently. *Ecology Letters*, **15**, 520–526.
Vogel JG, Bond-Lamberty BP, Schuur EAG *et al.* (2008) Carbon allocation in boreal black spruce forests across regions varying in soil temperature and precipitation. *Global Change Biology*, **14**, 1503–1516.
Warton DI, Wright IJ, Falster DS, Westoby M (2006) Bivariate line-fitting methods for allometry. *Biological Reviews*, **81**, 259–291.
Wolf A, Field CB, Berry JA (2010) Allometric growth and allocation in forests: a perspective from FLUXNET. *Ecological Applications*, **21**, 1546–1556.

Supporting Information

Additional Supporting Information may be found in the online version of this article:

Table S1. Data on gross primary production and soil respiration.
Table S2. Data on gross primary production and its components.
Table S3. Data used in principal component analysis and structural equation modeling.
Table S4. Reduced major axis regressions between GPP and its components.
Fig. S1. An *a priori* conceptual structural equation model.